International Conference on Mathematics, Computational Methods & Reactor Physics (M&C 2009)
Saratoga Springs, New York, May 3-7, 2009, on CD-ROM, American Nuclear Society, LaGrange Park, IL (2009)

A HYBRID MONTE CARLO-DETERMINISTIC APPROACH TO IMPROVE THE ACCURACY AND EFFICIENCY OF MONTE CARLO CALCULATIONS FOR THERMAL RADIATIVE TRANSFER

Allan B. Wollaber
Argonne National Laboratory
9700 S. Cass Ave. Argonne, IL 64039
awollaber@anl.gov

Edward W. Larsen
Department of Nuclear Engineering and Radiological Sciences
University of Michigan
2355 Bonisteel Blvd, Ann Arbor, Michigan 48109
edlarsen@umich.edu

ABSTRACT

A new hybrid Monte Carlo-deterministic method is presented to solve the nonlinear, frequency-dependent thermal radiative transfer (TRT) equations. Monte Carlo methods for radiative transfer typically treat temperature-dependent problem data by fixing it at the beginning of the time step, and variance reduction techniques have been limited in scope due to energy conservation requirements and the global problem nature. In the hybrid method presented here, a simpler system of gray, Quasidiffusion equations that contains average quantities supplied by the Monte Carlo solution over the previous time step is solved to provide approximate temperatures and scalar intensities for the upcoming Monte Carlo time step. The approximate temperature may be used to improve the accuracy of the temperature-dependent data evaluation or to adaptively select the time step size. The approximate gray scalar intensity may also be used to set the center of a weight window for variance reduction. We show that this approach can (i) enhance temporal convergence by reducing overshooting in the solution, (ii) ameliorate violations of the maximum principle in Marshak waves, and (iii) be much more efficient than Monte Carlo alone for some nonlinear (gray and frequency-dependent) sample problems.

Key Words: deterministic, Monte Carlo, hybrid, radiative transfer

1. INTRODUCTION

During the derivation of the Fleck and Cummings Implicit Monte Carlo (IMC) equations [1], some of the continuous-in-time problem data that depend on the material temperature – the opacities, specific heat, and the Planckian – are evaluated at the temperature at the beginning of the time step, T_n. The explicit-in-time treatment of these data introduces an error that worsens with increasing time intervals. Performing a time-extrapolation of the temperature using data from previous time steps has been used to try to lessen this error. However, such extrapolations are unreliable, as they can introduce new instabilities and additional errors into the calculation.

In this paper we present a new frequency-collapsed, deterministic Quasidiffusion [2, 3] method to estimate – before the IMC calculation is performed in each time step – the temperature and gray scalar intensity at the end of the time step. We also define a characteristic average

temperature T_* which properly interpolates the temperatures at the beginning and end of the time step, and which also can be used to evaluate the problem data.* This Quasidiffusion method is intended to be used in tandem with the more detailed transport calculation in the following manner.

- During the previous time step $t_{n-1} \leq t \leq t_n$, a frequency-dependent transport calculation such as IMC is carried out. Throughout this calculation, certain problem data are averaged over frequency and angle.
- These data are then provided to the new Quasidiffusion method, which uses them to estimate T_{n+1} for the upcoming time step $t_n \leq t \leq t_{n+1}$.
- The average temperature T_* is then generated and passed to the frequency-dependent transport algorithm, which then uses it to evaluate the temperature-dependent problem data.
- The Monte Carlo transport algorithm then produces solutions over the same time step $t_n \leq t \leq t_{n+1}$ using the more accurate problem data; these solutions supersede the Quasidiffusion solutions. The Monte Carlo transport algorithm can also use the Quasidiffusion estimate of the scalar intensity as the center of a weight window for variance reduction.

Concerning the weight window, Cooper and Larsen have previously suggested using the full forward solution $I(x, \mu, \nu, t)$ as a weight-window center, and they reported moderate success for gray radiative transfer problems [4]. However, extending their approach to frequency-dependent problems would be difficult to implement and would likely be computationally inefficient. A formal mathematical justification for our weight window center is as follows. The intensity I is related to the Monte Carlo number density M by:

$$I(x, \mu, \nu, t) = \int_0^\infty cwM(x, \mu, \nu, t, w)\, dw\,, \tag{1}$$

where w is the *energy-weight* of the Monte Carlo particle and c is the speed of light. An "infinitely-thin" weight-window centered on the exact frequency- and angle-integrated intensity implies that M be of the form:

$$M(x, \mu, \nu, t, w) = \hat{M}(x, \mu, \nu, t)\delta\left(cw - \langle I\rangle\,(x, t)\right)\,, \tag{2}$$

where we have used the angle bracket notation to indicate integration over all directions [μ] and frequencies [ν] and $\hat{M}$ is to-be-determined. Substitution of Eq. (2) into Eq. (1) gives:

$$\begin{aligned} I(x, \mu, \nu, t) &= \int_0^\infty cw\hat{M}(x, \mu, \nu, t)\delta\left(cw - \langle I\rangle\,(x, t)\right)\, dw\,, \\ \hat{M}(x, \mu, \nu, t) &= \frac{I(x, \mu, \nu, t)}{\langle I\rangle\,(x, t)}\,. \end{aligned} \tag{3}$$

If we integrate Eq. (3) over all angles and frequencies, we obtain:

$$\langle\hat{M}\rangle(x, t) = 1\,. \tag{4}$$

*The estimate of the upcoming temperature could be also used to adaptively select a time step size, although we do not implement this approach here.

Thus, the Monte Carlo particle density from this modified weight window center is uniform over space and time. Furthermore, Eq. (3) implies that the frequency-angle distribution of M should be proportional to the frequency-angle distribution of I. This implies that using a weight window center defined in Eq. (2) produces a scheme in which the frequency and angle distributions of the Monte Carlo particles is exactly matched to that of the physical problem ("physically important" photon frequencies match the "numerically important" Monte Carlo particle frequencies).

2. CONSISTENT, GRAY QUASIDIFFUSION EQUATIONS

In this paper we assume a 1-D spatial representation of the nonlinear, frequency-dependent transport problem, although (with one caveat) extension to multidimension should be straightforward. We begin from the exact TRT equations with the mindset of performing the fewest number of approximations necessary to arrive at a relatively simple – but hopefully accurate – algebraic system of equations for the temperature T. The 1-D, purely-absorbing, frequency-dependent TRT equations, suppressing the independent variables where it is clear, are:

$$\frac{1}{c}\frac{\partial I}{\partial t} + \mu\frac{\partial I}{\partial x} + \sigma I = 2\pi\sigma B\,, \tag{5a}$$

$$\frac{\partial U_m}{\partial t} = \int_0^\infty \int_{-1}^1 \sigma(I - 2\pi B)\, d\mu\, d\nu\,. \tag{5b}$$

In these equations, the unknowns are the specific intensity $I = I(x, \mu, \nu, t)$, the material energy density $U_m = U_m(x, t)$, and the "equilibrium" radiative energy density $U_r = U_r(x, t)$. The quantity $B = B(\nu, T)$ is the Planck spectrum. The material temperature T is related to the material energy density by the specific heat c_v:

$$\frac{\partial U_m}{\partial T}(x, t) = c_v(x, T)\,, \tag{5c}$$

and the equilibrium radiative energy density is related to the material temperature by:

$$U_r(x, t) = aT^4(x, t)\,. \tag{5d}$$

where $a = 0.0137$ jk/cc-keV^4 is the radiation constant. We denote a frequency and angular integration by:

$$\langle f\rangle = \int_0^\infty \int_{-1}^1 f(\mu, \nu)\, d\mu\, d\nu\,. \tag{6}$$

Then, we operate on Eq. (5a) by $\langle\cdot\rangle$ and rewrite Eq. (5b) as:

$$\frac{1}{c}\frac{\partial}{\partial t}\langle I\rangle + \frac{\partial}{\partial x}\langle\mu I\rangle + \langle\sigma I\rangle = 2\pi\langle\sigma B\rangle\,, \tag{7a}$$

$$c_v\frac{\partial T}{\partial t} = \langle\sigma I\rangle - 2\pi\langle\sigma B\rangle\,. \tag{7b}$$

The Planck opacity is denoted by:

$$\sigma_p(x) = \frac{\langle\sigma B\rangle}{\langle B\rangle}, \tag{8}$$

and we define the intensity-weighted opacity σ_I:

$$\sigma_I(x) = \frac{\langle\sigma I\rangle}{\langle I\rangle}\,. \tag{9}$$

Then Eqs. (7) become, using Eq. (9) and Eq. (8):

$$\frac{1}{c}\frac{\partial}{\partial t}\left\langle I\right\rangle + \frac{\partial}{\partial x}\left\langle \mu I\right\rangle + \sigma_I \left\langle I\right\rangle = \sigma_p caT^4 \,, \tag{10a}$$

$$c_v \frac{\partial T}{\partial t} = \sigma_I \left\langle I\right\rangle - \sigma_p caT^4 \,. \tag{10b}$$

Next, we multiply Eq. (5a) by μ/σ:

$$\frac{\mu}{c\sigma}\frac{\partial I}{\partial t} + \frac{\mu^2}{\sigma}\frac{\partial I}{\partial x} + \mu I = \mu 2\pi B \,, \tag{11}$$

and operate on the result with $\langle\cdot\rangle$:

$$\frac{1}{c}\left\langle \frac{1}{\sigma}\frac{\partial}{\partial t}\mu I\right\rangle + \left\langle \frac{\mu^2}{\sigma}\frac{\partial I}{\partial x}\right\rangle + \left\langle \mu I\right\rangle = 0 \,. \tag{12}$$

Here we make our first approximation – as is commonly done in diffusion approximations – and discard the time derivative of the first angular moment to find: [†]

$$\left\langle \mu I\right\rangle \approx -\left\langle \frac{\mu^2}{\sigma}\frac{\partial I}{\partial x}\right\rangle \,. \tag{13}$$

We use this relationship to eliminate the derivative of the first angular moment in Eq. (10a) by creating a frequency-averaged Eddington factor and a special, frequency-averaged opacity. From the above we may write

$$\begin{aligned}\frac{\partial}{\partial x}\left\langle \mu I\right\rangle &\approx -\frac{\partial}{\partial x}\left\langle \frac{\mu^2}{\sigma}\frac{\partial I}{\partial x}\right\rangle \,, \\ &= -\frac{\partial}{\partial x}\left\langle \frac{1}{\sigma}\frac{\partial}{\partial x}\frac{\mu^2 I}{\left\langle \mu^2 I\right\rangle}\left\langle \mu^2 I\right\rangle\right\rangle \,,\end{aligned}$$

but we make a further approximation that:

$$\frac{\partial}{\partial x}\frac{\mu^2 I}{\left\langle \mu^2 I\right\rangle} \approx 0 \,, \tag{14}$$

which is valid if I is nearly a separable function of space and angle or if I is a slowly-varying spatial function. Then,

$$\begin{aligned}\frac{\partial}{\partial x}\left\langle \mu I\right\rangle &\approx -\frac{\partial}{\partial x}\left\langle \frac{1}{\sigma}\frac{\mu^2 I}{\left\langle \mu^2 I\right\rangle}\right\rangle \frac{\partial}{\partial x}\left\langle \mu^2 I\right\rangle \,, \\ &= -\frac{\partial}{\partial x}\frac{\left\langle \frac{1}{\sigma}\mu^2 I\right\rangle}{\left\langle \mu^2 I\right\rangle}\frac{\partial}{\partial x}\frac{\left\langle \mu^2 I\right\rangle}{\left\langle I\right\rangle}\left\langle I\right\rangle \,, \\ &\equiv -\frac{\partial}{\partial x}\frac{1}{\sigma_\rho}\frac{\partial}{\partial x}E\left\langle I\right\rangle \,,\end{aligned} \tag{15}$$

where we have defined:

$$E(x) = \frac{\left\langle \mu^2 I\right\rangle}{\left\langle I\right\rangle} \,, \tag{16}$$

$$\sigma_\rho(x) = \frac{\left\langle \mu^2 I\right\rangle}{\left\langle \frac{\mu^2}{\sigma} I\right\rangle} \,. \tag{17}$$

[†] Note that this implies that the equations are no longer "flux-limited." For a discussion, see [5].

Here, E is a frequency-averaged Eddington factor. Also, σ_ρ is a specially-weighted opacity that, in the limit as I resembles a Planck function, almost produces the Rosseland mean opacity. In Eqs. (16) and (17) lie the caveat for the extension to multidimensions; the quantities E and σ_ρ will become angle tensors. The treatment for Eq. (16) is straightforward, but a slightly different approach may be necessary to obtain angle-dependent values in the derivation of σ_ρ in Eq. (15). We shall demonstrate numerically that the above approximations in Eq. (14) and Eq. (15) produce excellent results as a proof of principle, and we remark that additional approximations or a more complicated expression for σ_ρ could be considered in multidimensions.

Substituting Eq. (15), Eq. (16), and Eq. (17) into Eqs. (10), we arrive at a much simpler Quasidiffusive version of the TRT equations in which the frequency and angular variables have been eliminated.

$$\frac{1}{c}\frac{\partial}{\partial t}\langle I\rangle - \frac{\partial}{\partial x}\frac{1}{\sigma_\rho}\frac{\partial}{\partial x}E\langle I\rangle + \sigma_I\langle I\rangle = \frac{1}{2}\sigma_p c U_r\,, \tag{18a}$$

$$c_v\frac{\partial T}{\partial t} + \sigma_p c a T^4 = \sigma_I\langle I\rangle\ . \tag{18b}$$

Eqs. (18) are a central result of this paper. To deterministically solve Eqs. (18), we perform an implicit time discretization of their unknowns (for now, leaving the temperature-dependent quantities evaluated at $t = t_n$) to find:

$$-\frac{\partial}{\partial x}D_n\frac{\partial}{\partial x}E_n\langle I\rangle_{n+1} + \Sigma_n\langle I\rangle_{n+1} = S_n\,, \tag{19a}$$

$$U_{m,n+1} = U_{m,n} - \Delta_{t,n}f_n\sigma_{p,n}cU_{r,n} + \Delta_{t,n}f_n\sigma_{I,n}\langle I\rangle_{n+1}\ , \tag{19b}$$

where

$$f_n = \frac{1}{1+\beta_n\sigma_{p,n}c\Delta_{t,n}}\,, \qquad D_n = \frac{1}{\sigma_{\rho,n}}\,, \tag{19c}$$

$$\Sigma_n = \frac{1}{c\Delta_{t,n}} + f_n\sigma_{I,n}\,, \qquad S_n = f_n\sigma_{p,n}cU_{r,n} + \frac{1}{c\Delta_{t,n}}\langle I\rangle_n\ . \tag{19d}$$

The temperatures T_{n+1} are updated by solving:

$$U_{m,n+1} = \int_0^{T_{n+1}} c_v(T')\,dT'\,. \tag{19e}$$

The next step would be to spatially discretize Eqs. (19); for this we used a standard finite-volume spatial representation (for details, see [5]).

3. SOLUTION PROCEDURE

In a general time step, an IMC calculation is carried out in which the quantities E_n, σ_{ρ_n}, and $\sigma_{I,n}$ are tallied. These data are then supplied to a deterministic solver for Eqs. (19), which produces estimates of the temperature and gray scalar intensity at the end of the upcoming time step. The IMC calculation for the upcoming time step may then exploit this data for variance reduction and temperature-evaluation purposes. We next describe some of the details that affect the accuracy and performance of our implementation.

3.1. An Average Interpolated Temperature

For sufficiently small time steps, the time-dependence of the temperature is approximately linear:

$$T(t) \approx T_n + \frac{T_{n+1} - T_n}{\Delta_t} t \,. \tag{20}$$

Then, assuming an opacity of the form

$$\sigma = \frac{\gamma}{T(t)^3} \,, \tag{21}$$

we look for a time-averaged σ given by:

$$\overline{\sigma} = \frac{1}{\Delta_t} \int_{t_n}^{t_{n+1}} \frac{\gamma}{T(t)^3} \, dt = \frac{\gamma}{T_*^3} \,, \tag{22}$$

where T_* is the properly averaged, time-dependent temperature at which to evaluate the opacities. Substituting Eq. (20) into Eq. (22) and carrying out this integral, we obtain:

$$\frac{1}{T_*^3} = \frac{(T_{n+1} + T_n)/2}{T_n^2 T_{n+1}^2} \,,$$

or

$$T_* = \left(\frac{T_n^2 T_{n+1}^2}{(T_{n+1} + T_n)/2} \right)^{1/3} \,. \tag{23}$$

Using the temperature defined by Eq. (23) to evaluate the opacities in an IMC calculation is more accurate than using T_n. In addition to the opacities, there are other temperature-dependent factors that appear in the IMC equations, specifically, $b_n(\nu)$, β_n, and f_n. Although these do not contain a temperature dependence of T^{-3}, in this paper, these will also be evaluated at the temperature T_*. One reason for doing this is consistency – if one attempts to use a different temperature to evaluate the normalized Planck function $b_n(\nu)$ and/or β_n, this would necessitate the introduction of an emission spectrum that depends on more than one temperature. This is possible to do, but inconvenient. Additionally, since the equation for $U_r(t)$ contains the product $\sigma_p \beta$, then under the usual assumption that c_v is constant,

$$\sigma_p \beta = \frac{\gamma}{T^3} \frac{4aT^3}{c_v} = \text{ constant} \,. \tag{24}$$

Thus, evaluating β and σ_p at the same temperature ensures that this product remains constant. Since the Fleck factor f contains this product, this also implies that $f_* = f_n$. However, as future work, alternative treatments of temperature-dependence of $b(\nu)$ and β should be considered. For instance, different average temperatures could be defined and independently used to evaluate the opacities, β, and the normalized Planck function. In this paper, we use T_* to evaluate all of the temperature-dependent problem data with the expectation that this should be an improvement over the use of T_n, and the acknowledgment that it is likely possible to further improve the IMC calculation by defining alternative time-averaged temperatures.

3.2. Iterative Refinement and Adaptivity

As it is *much* less numerically expensive to perform the deterministic, gray, Quasidiffusion calculation than the corresponding IMC calculation, it is feasible to iteratively refine the estimate of T_{n+1}. It is known that the Planck and Rosseland mean opacities are proportional to T^{-3}. Let us further assume that σ_I and σ_ρ contain this proportionality. If this is true, then instead of freezing the opacities to their known values at the beginning of the time step, a more accurate result may be obtained by using estimated opacities that have been averaged over the time step. We define an iteration index i and "time-averaged" opacities:

$$T_*^{(i)} = \left(\frac{T_n^2 (T_{n+1}^{(i)})^2}{(T_{n+1}^{(i)} + T_n)/2} \right)^{1/3} , \tag{25a}$$

$$\sigma_{\rho,*}^{(i)} = \sigma_{\rho,n} \left(\frac{T_n}{T_*^{(i)}} \right)^3 , \tag{25b}$$

$$\sigma_{I,*}^{(i)} = \sigma_{I,n} \left(\frac{T_n}{T_*^{(i)}} \right)^3 , \tag{25c}$$

$$\sigma_{p,*}^{(i)} = \sigma_{p,n} \left(\frac{T_n}{T_*^{(i)}} \right)^3 , \tag{25d}$$

and a time-averaged β by:

$$\beta_*^{(i)} = \beta_n \left(\frac{T_*^{(i)}}{T_n} \right)^3 . \tag{25e}$$

The quantities in Eqs. (25) are initialized at $i = 0$ by setting $T_*^{(i)} = T_n$. Using these definitions, we rewrite Eqs. (19) with iteration index i as:

$$D_*^{(i)} = \frac{1}{\sigma_{\rho,*}^{(i)}} , \tag{26a}$$

$$\Sigma_*^{(i)} = \frac{1}{c\Delta_{t,n}} + (f\sigma_I)_*^{(i)} , \tag{26b}$$

$$S_*^{(i)} = (f\sigma_p)_*^{(i)} c U_{r,n} + \frac{1}{c\Delta_{t,n}} \langle I \rangle_n . \tag{26c}$$

Then Eq. (19a) may be rewritten using Eqs. (26) as:

$$-\frac{\partial}{\partial x} D_*^{(i)} \frac{\partial}{\partial x} E_n \langle I \rangle_{n+1} + \Sigma_*^{(i)} \langle I \rangle_{n+1} = S_*^{(i)} , \tag{27a}$$

for iteration index i, and its solution may be used to solve an iterative version of Eq. (19b):

$$U_{m,n+1}^{(i+1)} = U_{m,n} - (f\sigma_p)_*^{(i)} c U_{r,n} + (f\sigma_I)_*^{(i)} \langle I \rangle_{n+1} . \tag{27b}$$

Finally, inverting

$$U_{m,n+1}^{(i+1)} = \int_0^{T_{n+1}^{(i+1)}} c_v(T')\, dT' \tag{27c}$$

provides $T_{n+1}^{(i+1)}$, which may be used to update the quantities $D_*^{(i+1)}$, $\Sigma_*^{(i+1)}$ and $S_*^{(i+1)}$ for the next iteration. This process can be repeated until T_{n+1} has converged and does not require many iterations. We note that this iterative procedure is not critical; we have experimentally found that one "iteration" is enough to make a substantial difference in solution accuracy.

If the time steps are sufficiently large, then it is possible for Eq. (27b) to produce non-physical, negative values of $U_{m,n+1}$. Such behavior can be guarded against by ensuring that [from Eq. (27b)]:

$$U_{m,n} \geq \Delta_t f_* \sigma_{p,*} c U_{r,n} \,. \tag{28}$$

Since f is a monotonically decreasing function of Δ_t and

$$\lim_{\Delta_t \to \infty} \frac{\Delta_t}{1 + \beta_* \sigma_{p,*} c \Delta_t} = \frac{1}{\beta_* \sigma_{p,*} c} \,, \tag{29}$$

it is sufficient to satisfy

$$U_{m,n} \geq \frac{1}{\beta_* \sigma_{p,*} c} \sigma_{p,*} c U_{r,n} = \frac{1}{\beta_*} U_{r,n} \,, \tag{30}$$

or

$$\beta_* \geq \frac{U_{r,n}}{U_{m,n}} \,. \tag{31}$$

For the case in which $c_v =$ constant, this may be written as:

$$\frac{4aT_*^3}{c_v} \geq \frac{aT_n^4}{c_v T_n} \,, \tag{32}$$

or

$$T_* \geq T_n \left(\frac{1}{4}\right)^{1/3} \approx 0.63 T_n \,. \tag{33}$$

Both the Quasidiffusion and IMC equations require this restriction on T_*; one is not free to use arbitrary temperatures to evaluate the problem data. During the IMC calculation, we explicitly enforce Eq. (33) – if the Quasidiffusion method produces a value of T_* that violates Eq. (33), then T_* is increased so that it satisfies Eq. (33). Eq. (33) represents a limit on the numerical cooling rate. It is noteworthy that a stronger limit also exists in the standard IMC equations since the maximum amount of radiation released from the material is (assuming c_v constant):

$$\lim_{\Delta_t \to \infty} \Delta_t f_n \sigma_{p,n} c U_{r,n} = \frac{c_v}{4} T_n = \frac{1}{4} U_{m,n} \leq U_{m,n} \tag{34}$$

This deficiency may contribute to the failure of IMC to contain the equilibrium diffusion limit (see [6]).

The general conclusion is that one should exercise caution if the temperature estimation scheme predicts temperatures that are substantially different from T_n, as this indicates that the desired time step is too large. Alternatively, this property of the temperature estimation algorithm could be used to adaptively reduce the size of the time step. For instance, if Eq. (33) is not satisfied, or if the temperature is predicted to change beyond some user-specified factor, one could search for a shorter time step size that produces an acceptable value of T_*. In current

implementations of the IMC procedure that do not have access to this methodology, there is no way to determine if a proposed time step is too large until after the calculation has ended. Employing a Quasidiffusion calculation to estimate the maximum time step size before the IMC calculation is performed could be a relatively inexpensive way to circumvent this difficulty.

3.3. Weight Window Implementation

To implement weight windows into IMC, a special form of the so-called "Russian roulette" variance reduction procedure is employed. For traditional Russian roulette, we define w_{low} to be a lower energy-weight cutoff and w_{avg} to be the desired average energy-weight. Then if a particle with energy-weight w undergoes a collision and $w < w_{\text{low}}$, with probability $p = w/w_{\text{avg}}$ (a relatively low probability) we increase the particle's energy weight to w_{avg}, and with probability $(1-p)$ (a relatively high probability), we terminate the particle history. [‡] This technique does not conserve energy since, with probability p, the energy $w_{\text{avg}} - w$ is created "from nowhere", and with probability $(1-p)$ the energy w is lost. To conserve energy, we modify this procedure by introducing a position-dependent "bank" of rouletted energy. In this scheme, when a particle is terminated, its energy-weight is deposited into the energy bank. If a particle's energy is to be increased, its increase is restricted to the amount available in the energy bank. At the end of the calculation if excess energy remains in the bank (and this quantity is usually small), then it is deposited in the material. If too-few particles are used, then it is possible that this technique may introduce an inaccuracy into the problem, since the energy bank does not account for the location or time at which energy becomes available.

In our test code, we nominally set the spatially-dependent weight window center (as did Cooper and Larsen using a different Quasidiffusion procedure [4]) using:

$$w_c(x) = \langle I \rangle_{n+1} \ , \tag{35}$$

where the estimate of $\langle I \rangle_{n+1}$ is provided from the Quasidiffusion solution. This weight window center is of the form depicted in Eq. (2); the only difference is that the scalar intensity generated from the temperature estimation algorithm is approximate. This is permissible so long as the weight window center is sufficiently accurate to capture the spatial and temporal variation of the IMC intensity solution, and the width of the weight window is large enough to accommodate any errors. Generally, more accurate weight window centers should produce more efficient Monte Carlo solutions.

For a generic TRT problem in which accurate solutions are sought throughout the entire spatial domain, Eq. (35) should be expected to increase the efficiency of the IMC calculation (provided that the weight window width is properly chosen). However, certain TRT problems exist in which accurate solutions are *not* desired throughout the entire spatial domain of the problem. One example of this is Marshak wave problems. These problems can be divided into three regions: (1) the region behind the wavefront, in which the spatial gradient of the temperature solution is small, (2) the region in the vicinity of the wavefront, in which the temperature solution varies rapidly, and (3) the region ahead of the wavefront, in which the gradient is small and the problem is generally in near-equilibrium at the initial temperature. Accurate temperature

[‡] Note that in our test code, we do not employ the continuous energy deposition variance reduction technique, opting instead for an implicit capture procedure, necessitating the calculation of a collision location.

solutions are sought in regions 1 and 2, in which the temperature wave has already propagated through and is propagating, respectively. Ahead of the wavefront, in region 3, relatively unimportant problem physics is occurring (if the spatial boundary is vacuum, some cooling may occur, otherwise region 3 is relatively slowly being heated by high-frequency photons).

Using a weight window center $w_c(x) = \langle I \rangle_{n+1}(x)$ treats all of the spatial regions with equal importance, as may be seen in Eq. (4). This is undesirable, especially when particles moving from the relatively high-density regions 1 or 2 reach region 3, where they would typically be forced to undergo computationally-intensive particle splitting. However, we can capitalize on this *a priori* knowledge of the TRT problem by modifying the weight window in advance to prevent the potential "waste" of computational resources in region 3.

We define $w_{\min}$ as the minimum weight window center to be used in the problem. For a Marshak wave problem, this usually corresponds to the initial problem temperature, in which case,

$$w_{\min} = acT_i^4 \,. \tag{36}$$

We would like to avoid excessive particle tracking (especially splitting) in spatial zones for which $w_c(x) \approx w_{\min}$, as these zones may usually assumed to be near equilibrium (in region 3). We therefore propose the following modification to the weight window generated from the above algorithm:

$$w_{\mathrm{m}}(x) = w_c(x)\left[1 + \left(\frac{1}{\epsilon} - 1\right) e^{-(w_c(x) - w_{\min})/\epsilon}\right] \,. \tag{37}$$

We note that ϵ appears twice in Eq. (37). One could consider using different values in each location, but we did not. We note that if ϵ is not sufficiently small, then the modified weight window may inadvertently "clip" weights that are relatively large compared to the minimum weight. If ϵ is chosen to be very small, then the continuous function begins to approach a δ function at the lower weight cutoff, which essentially introduces a discontinuity. For our numerical problems, we set $\epsilon = 0.01$. Figure 1 depicts an example of modified weight windows $w_m(x)$ with $\epsilon = 0.05$, $\epsilon = 0.01$, and $\epsilon = 0.001$, and the unmodified weight window $w_c(x) = \langle I \rangle (x)$. The example unmodified weight window $w_c(x)$ was numerically generated by the deterministic Quasidiffusion solution in a gray, dimensionless Marshak wave problem with $\Delta_x = 0.025$ and $\Delta_\tau = 0.1$ at a time midway in the IMC calculation. For this problem, the initial scalar intensity – and $w_{\min}$ – are 0.0001. In Figure 1, each of the modified weight windows successfully raises the weight window center in the region ahead of the wavefront (region 3). This implies that there should be fewer Monte Carlo particles in region 3. Decreasing the value of ϵ increases the modified weight window throughout region 3. We also observe that decreasing the value of ϵ changes the rapidity with which the modified weight windows change in the vicinity of the wavefront (region 2). This is an important characteristic, as it affects the Monte Carlo particle density in region 2. For $\epsilon = 0.05$, $w_m(x)$ begins to increase somewhat early in region 2. This is undesirable, as it would decrease the amount of Monte Carlo particles there. When $\epsilon = 0.01$ (which is the value that we use in our numerical calculations), the weight window increase begins to occur at the leading edge of the wavefront. When $\epsilon = 0.001$, the weight window increase also occurs at the leading edge of the wavefront, but it is more dramatic in that it rapidly climbs to a value that is comparable to the weight window behind the wavefront (region 1). None of the modified weight windows has a discernible effect in region 1.

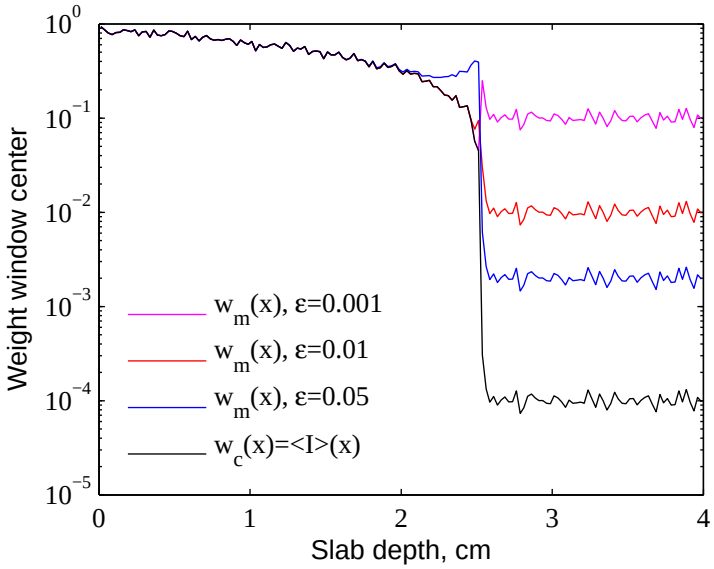

Figure 1. The Unmodified Weight Window Center $w_c(x) = \langle I \rangle (x)$ and Modified Weight Window Centers $w_m(x)$ for $\epsilon = 0.05$, 0.01, and 0.001 for an Example Marshak Wave Problem With an Initial Scalar Intensity of 0.0001.

We note that Cooper proposed a similar modification to his weight window in gray Marshak wave problems in his thesis [4]. His modification is to raise the *top* of the weight window to "infinity" (any value large enough to eliminate splitting) whenever the predicted temperature solution is less than 105% of the initial temperature:

$$T_{n+1}(x) \leq 1.05\ T(x,0)\,.$$

Our proposed modification is different in that (i) it is spatially-continuous, and (ii) the *center* of the weight window is adjusted. Therefore, our modification reduces the probability of particle splitting and increases the probability of Russian roulette in region 3, whereas Cooper's modification only eliminates splitting. Later in his thesis, Cooper remarked that his modification may be "too crude." [4] We believe that our proposed modification represents an advancement, but it is likely not optimal.

4. NUMERICAL RESULTS

In these results, we refer to the ordinary IMC method simply as IMC, to IMC with temperature-dependent data evaluated at T_* as IMC-T_*, to the IMC method with a weight window as IMC-WW, and to the combination as IMC-WW-T_*. The "modified" weight window method is denoted by IMC-MWW.

4.1. Accuracy Improvements

We begin by numerically demonstrating the potential accuracy gains by using the IMC-T_* approach for a gray, 0-D, nonlinear problem and for a gray, 1-D, Marshak wave problem.

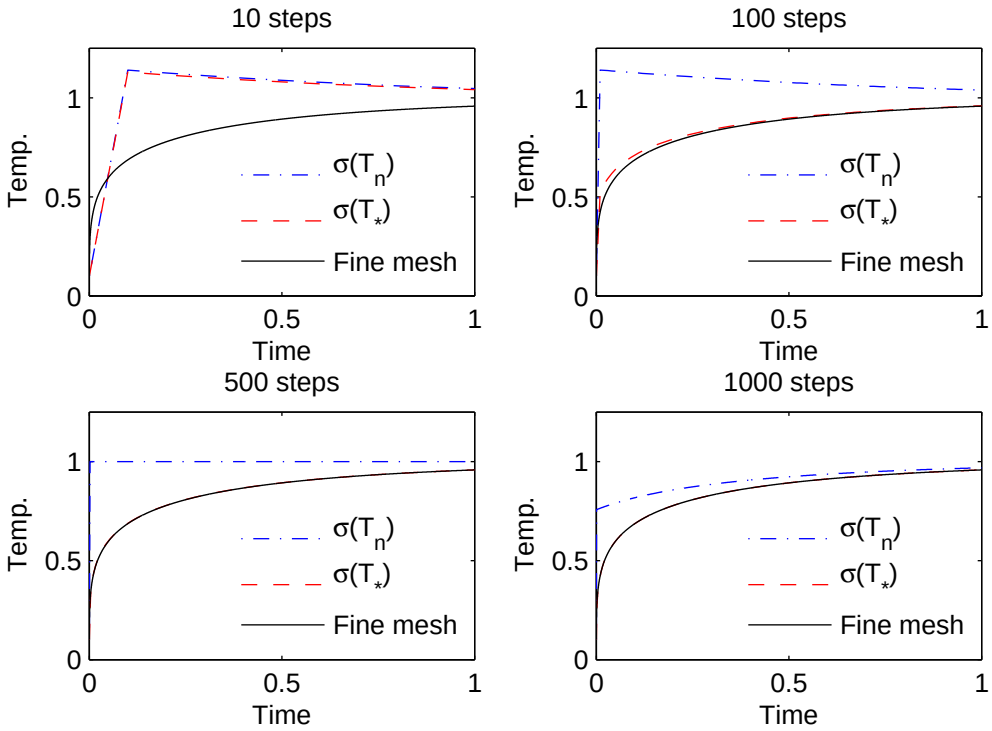

Figure 2. The Time-Dependent Temperatures for IMC Methods That Use Data Evaluated at T_n (Blue) and at T_* (Red) for 10, 100, 500, and 1000 Time Steps.

4.1.1. A 0-D nonlinear problem

To numerically assess the temporal accuracy gains of the IMC-T_* method, we first consider a sample 0-D problem that employs the gray, nonlinear TRT equations. For this problem, we assume that $\sigma = T^{-3}$, $a = c = 1$, and $c_v = 7.14$. The temperature is set to an initial condition of 0.1, and the initial intensity ϕ is 7.428. The problem is solved using a variable number of time steps with an ending time fixed at $t = 1$, at which point the fine-mesh temperature solution is 0.96 [the temperature is 96% converged to its specified equilibrium condition].

Figure 2 depicts the time-dependent temperatures for the IMC-T_* and traditional IMC methods using a variable number of time steps. From Figure 2, we determine that if 10 time steps are used, then both solutions overshoot the equilibrium condition and begin monotonic decay. If 100 time steps are used, then the IMC solution that uses data at T_n continues to overshoot the solution, but the IMC-T_* solution nicely approximates the fine-grid solution. Even if as many as 1000 steps are used, the traditional IMC solution continues to overshoot the equilibrium solution, while the IMC-T_* solution becomes indiscernible from the fine-grid solution. This overshooting in the traditional IMC equations is an undesirable characteristic that is discussed in [7], but the use of T_* ameliorates this issue.

4.1.2. Gray, nonlinear Marshak waves

In Wollaber's Ph.D. thesis [5], a numerically difficult nonlinear, gray Marshak wave problem is prescribed, analyzed, and solved using different approaches. This problem is described by using dimensionless variables obtained by setting $a = c = 1$, $c_v = 7.14$, $\sigma = T^{-3}$, and introducing the scaled time variable $\tau = (ac/c_v)t$. [§] The initial temperature is 0.1. We impose an isotropic right boundary condition equal to the initial temperature and an isotropic left boundary condition at 1.0. We consider a slab that is 4 cm wide. This implies that the slab is initially 4,000 mean free paths thick, but only 4 mean free paths thick once equilibrium is reached. We track the wavefront up to $\Delta_\tau = \Delta_t/c_v = 40$. The spatial grid and time step sizes are varied, and each problem is solved using a Monte Carlo algorithm.

The IMC solutions at the fixed time $\tau = 8$ are presented for variable cell sizes in Figure 3(a) and variable time step durations in Figure 3(b). In each of these figures we can see the worsening violations of the maximum principle [8] that result from increasing Δ_τ or decreasing Δ_x. Note that, because these figures are all depict temperature solutions at the *same* solution time, the "flattest" and right-most wave profile in each figure is the most accurate – ideally all the wave profiles should match this. The corresponding IMC-T_* wavefronts are provided as Figures 3(c) and 3(d) below their corresponding IMC solutions for ease of comparison. In the IMC-T_* solutions we observe that (i) the degree of maximum principle violation is reduced or eliminated in some cases, and (ii) the wavefront location is more accurate. We also observe that in the extreme cases, a spatial oscillation is introduced just behind the wavefront. This is an unphysical feature of the solution, but the gain in accuracy likely outweighs its existence. As mentioned earlier, the Quasidiffusion calculation can also be used to predict this behavior and limit the upcoming time step size.

4.2. Efficiency Improvements

We next consider using global weight windows on a frequency-dependent Marshak wave problem. In this problem, $c \approx 300$ cm/sh and $a = 0.01372$ jk/cm^3-keV^4. The initial condition is an equilibrium state with $T = 0.01$ keV. At $t = 0$, the left side of the slab is subjected to an isotropic burst of radiation at temperature $T = 1$ keV. The right boundary temperature is set to the constant, initial temperature. The slab size is 4 cm thick. The opacity is given by:

$$\sigma_a(\nu, T) = \frac{200}{(h\nu)^3}\left(1 - e^{-h\nu/T}\right) , \tag{38}$$

The Planck mean opacity is therefore $30.8T^{-3}$ which means, at equilibrium ($T = 1$), the slab is 123.2 Planck mean free paths thick, whereas at the initial condition $T = 0.01$, it is 123.2 $\times 10^6$ Planck mean free paths thick. The specific heat is set to 0.1 jk/keV-cc. We consider temperature solutions up to 1 sh. The spatial grid size Δ_x is set to 0.2 cm. The upper weight window cut-off is $10w_c(x)$; the lower cut-off is $0.1w_c(x)$.

This problem was simulated using 100,000 particles/jk. To estimate relative errors and calculate figures of merit, the problem was independently simulated 50 times; the relative errors

[§] For more background on this scaling, we refer the reader to a companion paper on stability or to [5].

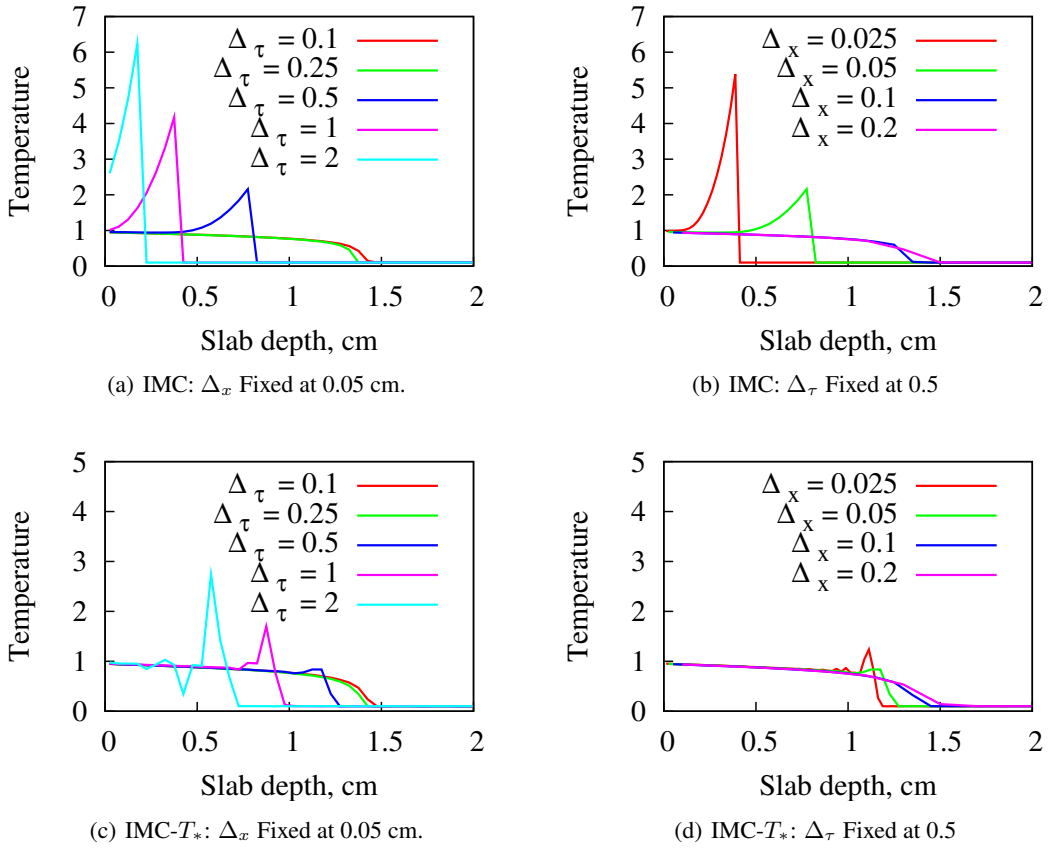

(a) IMC: Δ_x Fixed at 0.05 cm.

(b) IMC: Δ_τ Fixed at 0.5

(c) IMC-T_*: Δ_x Fixed at 0.05 cm.

(d) IMC-T_*: Δ_τ Fixed at 0.5

Figure 3. Temperature Profiles at $\tau = 8$ for a Marshak Wave Problem in which [(a), (c)] the Time Step is Varied and [(b), (d)] the Spatial Grid Size is Varied Using "Traditional" IMC (Above) and IMC-T_* (Below).

were then calculated using the sample error. To compare the solution efficiencies, we employ the figure of merit (FOM), defined by:

$$FOM(x,t) = \frac{1}{R(x,t)^2 t_{\text{cpu}}}, \tag{39}$$

where, R is the relative error in the estimate of the solution at position x and time t, and t_{cpu} is the total calculation time (including the deterministic calculation) required to generate the solution at time t.

Using a time step of $\Delta_t = 0.001$ sh, the above-described frequency-dependent problem was simulated using the IMC, IMC-MWW, and IMC-MWW-T_* methods. It was not possible to obtain solutions using the IMC-WW method (the method that uses an unmodified global weight window). When the IMC-WW method was attempted for this problem, the requested memory to follow the daughter particles due to particle splitting exceeded the available memory on the machines. This demonstrates that weight windows generated for an assumed-global problem should not blindly be applied to a sufficiently difficult problem that is truly only semi-global in nature (i.e., the region ahead of the wavefront does not fundamentally affect the problem

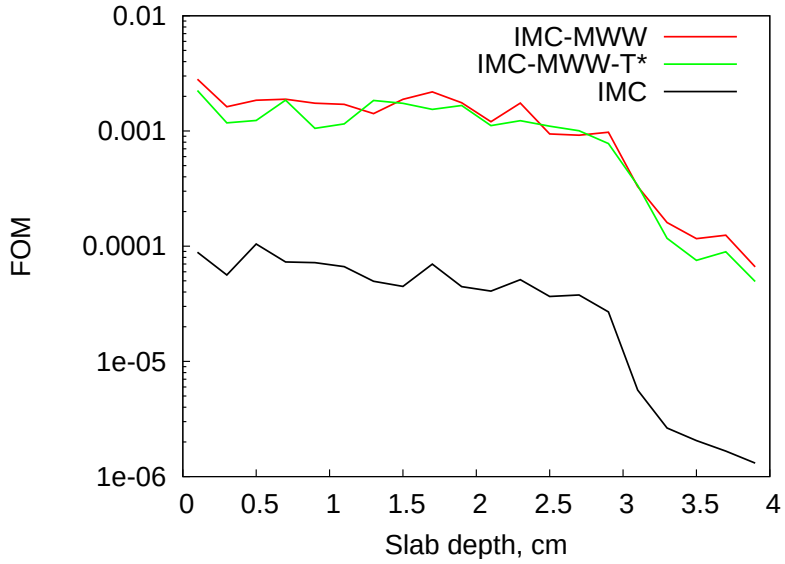

Figure 4. Temperature-FOM Profile at $t = 0.9$ sh for a Frequency-Dependent Marshak Wave Problem Solved Using the IMC, IMC-MWW, and IMC-MWW-T_* Methods with $\Delta_t = 0.001$.

solution). For this problem at least, it is necessary to restrict the application of the weight window only to regions where the Marshak wave is expected to be.

Figure 4 depicts the temperature-FOMs at $t = 0.9$ sh for the IMC, IMC-MWW, and IMC-MWW-T_* methods. We note that the deterministic solution time is included in the FOM. In general, the weight window methods are at least an order of magnitude superior to the IMC method. This difference is mostly attributable to differences in computation times, since the "traditional" IMC method, without Russian roulette, is handicapped by its inability to dispose of low-weight particles. This is an encouraging result, given that the problem is numerically difficult and the deterministic Quasidiffusion method and weight window modification logic are relatively simple. This suggests that these results could likely be further improved.

4.3. Implementation Issues

Two difficulties were encountered during the solution of the frequency-dependent problem that are worth reporting. The first concerns the Monte Carlo estimator of σ_ρ defined in Eq. (17). The direct definition leads to undesirable statistical noise in the temperature estimate, and to a lesser degree, the interpolation temperature T_*, although this did not appear to affect the overall solution accuracy. The estimator includes the factor $1/\sigma(\nu)$; when a high-frequency particle contributes to the tally (corresponding to an exponentially small opacity), this factor can become very large. These relatively rare "spikes" in the tally can significantly increase the variance in the Monte Carlo estimator of σ_ρ, which introduces noise into the Quasidiffusion temperature estimate.

To suppress this noise, we suggest using the following modification to the definition of σ_ρ:

$$\sigma'_\rho = \frac{\left\langle \frac{\sigma(\nu)}{\epsilon+\sigma(\nu)}\mu^2 I \right\rangle}{\left\langle \frac{\mu^2}{\epsilon+\sigma(\nu)} I \right\rangle}. \tag{40}$$

with ϵ set to be some small quantity. This has the following effect. When ν is small, $\sigma(\nu)$ is typically large. In this case, the numerator and denominator essentially reduce to the original form of σ_ρ seen in Eq. (17). When ν is large, $\sigma(\nu)$ can become exponentially small. However, the presence of ϵ in σ'_ρ now limits the tally contribution to $1/\epsilon$.

The second difficulty concerns the implementation of Russian roulette. In one of the problems, the leading edge of the IMC-MWW radiation wave was found to be slightly advanced with respect to the IMC solution. Upon inspection, this was found to be caused by using a zone-wide energy bank that does not account for the location of a particle "death," allowing for the unphysical conduction of "resurrected" particles. This can easily be remedied by using better logic for these tallies. However, time constraints prevented us from attempting either of these remedies.

5. CONCLUSIONS

In this paper we have presented a new method to estimate the end-of-time-step temperature T_{n+1} and gray, scalar radiation intensity $\langle I \rangle_{n+1}$ for nonlinear, frequency-dependent problems. Beginning from the 1-D, frequency-dependent form of the TRT equations, we derived new deterministic, gray, Quasidiffusion equations. In these equations we defined a new frequency-averaged Eddington factor E, and two new angle- and frequency-averaged opacities, σ_I and σ_ρ. The gray Quasidiffusion equations are *much* easier to solve than the original, frequency-dependent transport equation, and they should remain reasonably accurate since they exploit data generated from the transport solution during the previous time step. We then applied temporal and a finite-volume based deterministic scheme to solve them, with or without iteration on the temperature-dependent problem data. We also derived an appropriate time-average temperature T_* in Eq. (23).

We introduced a global angle- and frequency-independent weight window based on the deterministic, gray, (forward) Quasidiffusion equations. Using this weight window in a global TRT calculation helps to globally redistribute the particles throughout the spatial problem domain, decrease the required computational time, and increase the figures of merit in the temperature and radiation solutions. We motivated the use of a forward weight window by using the Monte Carlo number density. We showed that setting a weight window center to be proportional to the full forward problem solution implies a uniform Monte Carlo particle number density. We then argued that a superior solution for TRT problems is to set the weight window to be proportional to only the space-time elements of phase space (not frequency or angle). We also introduced a simple modification to the weight window to improve the efficiency of Marshak wave problems.

We numerically demonstrated that using T_* to evaluate the temperature-dependent quantities in an IMC calculation can lead to much more accurate solutions for a nonlinear, gray 0-D problem

and a 1-D Marshak wave problem. The Marshak wave solution was shown to be less susceptible to a violation of the maximum principle [8] and to have more accurate wavefront locations.

By solving a nonlinear, frequency dependent Marshak wave problem, we showed that substantial gains in efficiency can be obtained over "traditional" IMC by using our modified weight window. Two implementation issues were encountered with regard to statistical noise in the Monte Carlo estimator for σ_ρ and artificial conduction in Russian roulette, but these can be remedied as future work.

There are a considerable number of directions that might be taken as future work. A relatively inexpensive estimate of the upcoming end-of-time step temperature and scalar radiation intensity could allow one to: (i) adaptively control the time step size (in either deterministic or Monte Carlo codes), (ii) determine new temperature interpolation strategies to optimize accuracy, (iii) design optimized weight window controls for more general TRT problems, and (iv) perform dynamic domain decomposition in a parallel solution scheme. Extending this work to multidimensional space should be straightforward with the caveat that the Eddington factor E will become a tensor and either a more complicated expression or an additional approximation is necessary for σ_ρ [see Eqs. (16) and (17)].

In conclusion, the deterministic Quasidiffusion method presented in this chapter is a promising first step. The numerical results obtained by using this approach indicate a marked improvement over traditional IMC, and there are several reasons suggesting that further improvement could be obtained.

6. ACKNOWLEDGMENTS

This research was performed under appointment by the Department of Energy Computational Science Graduate Fellowship, which is provided under grant number DE-FG02-97ER25308.

REFERENCES

[1] J. A. Fleck, J. D. Cummings, "An Implicit Monte Carlo Scheme for Calculating Time and Frequency Dependent Nonlinear Radiation Transport," *J. of Comput. Phys.*, **8**, pp. 313–342 (1971).

[2] V. Y. Gol'din, "A Quasi-Diffusion Method of Solving the Kinetic Equation," *USSR Computational Mathematics and Physics*, **4**, pp. 136–149 (1967).

[3] D. Y. Anistratov, V. Y. Gol'din, "Nonlinear Methods for Solving Particle Transport Problems," *Transport Theory and Statistical Physics*, **22**, pp. 125–163 (1993).

[4] M. Cooper, *An Automated Variance Reduction Method for Global Monte Carlo Neutral Particle Transport Problems*, Ph.D. thesis, University of Michigan (1999).

[5] A. Wollaber, *Advanced Monte Carlo Methods for Thermal Radiation Transport*, Ph.D. thesis, University of Michigan (2008).

[6] J. D. Densmore, E. W. Larsen, "Asymptotic Equilibrium Diffusion Analysis of Time-Dependent Monte Carlo Methods for Grey Radiative Transfer," *J. Comput. Phys.*, **199**, pp. 175–204 (2004).

[7] N. Gentile, "A Comparison of Various Temporal Discretization Schemes for Infinite Media Radiation Transport," *Trans. Am. Nucl. Soc.*, **97**, pp. 544–546 (2007).

[8] E. W. Larsen, B. Mercier, "Analysis of a Monte Carlo Method for Nonlinear Radiative Transfer," *J. Comput. Phys.*, **71**, pp. 50–64 (1987).